

Emergence of structural anisotropy in Optical Glasses treated to support Second Harmonic Generation

C. Cabrillo, G.J. Cuello, P. García-Fernández and F.J. Bermejo
Instituto de Estructura de la Materia, Serrano 123, Madrid E-28006, Spain

V. Pruneri and P. G. Kazansky
*Optoelectronics Research Centre, University of Southampton,
Southampton SO17 1BJ, United Kingdom*

S.M. Bennington, W.S. Howells
Rutherford Appleton Laboratory, Chilton, Didcot, Oxon, OX11 0QX, United Kingdom
(November 19, 2018)

Structural alterations in $v\text{-SiO}_2$ induced by "thermal poling", a treatment which makes the glass able to double the frequency of an impinging infrared light, are revealed by neutron diffraction as a breakdown of the macroscopic isotropy. This leads to concomitant changes in the vibrational density of states measured by inelastic neutron scattering. The observations are found to be consistent with the emergence of partial ordering within the glassy matrix along the direction of an electrostatic field applied during the poling treatment.

61.12.-q, 81.40.-z, 42.70.Ce, 42.65.Ky

Few discoveries have puzzled the optics community more than the emergence of visible (green) light from optical fibers after strong irradiation by an infrared laser [1]. This frequency-doubling phenomenon known as Second Harmonic Generation (SHG) is not expected to take place in a centrosymmetric material such as the amorphous silica fiber-core, which shows no measurable second-order optical susceptibility $\chi^{(2)}$ [2]. The process to be efficient also requires well defined phase-matching between the interacting waves to allow for constructive interference, and this seems even more difficult to fulfill within the glassy medium. Several plausible explanations about the origin of the phenomenon have been put forward. One of the most widely accepted [3] does not involve structural modifications to accomplish the breakdown of the glass radial symmetry. Rather, it postulates the emergence of a spatially modulated local dc field, E_0 , which, via a third-order nonlinearity ($\chi^{(3)}$) (finite in isotropic materials), induces a spatially modulated second order nonlinearity ($\chi^{(2)} \propto \chi^{(3)} E_0$) able to double the pump frequency. The achievement of a permanent $\chi^{(2)}$ in optical glasses has focused a large research effort, which lead to the discovery of alternative poling techniques. In actual fact, the phenomenon can be produced by application of a high voltage (~ 5 kV, just below dielectric breakdown) to glass plates at moderate temperatures (~ 540 K – 580 K, compared with ≈ 1475 K where the glass melts). This method, known as "thermal" poling [4], provides permanent second-order nonlinear responses comparable to those shown by inorganic crystals. Whether the mechanism(s) leading to the emergence of a second order nonlinearity in "thermally-poled" glasses differ from those of photoinduced SHG or not needs to be clarified. At any rate, the relevant point stems from the possibility this method has opened up for developing inexpensive integrated optical frequency converters and electro-optic modulators.

Up to now studies on the microscopic structure and/or dynamical alterations associated with poling are scarce. Significant changes between poled and native fibers at rather well defined frequencies have been reported from Raman studies [5]. Direct interpretation of such Raman data is however hampered by the need of knowledge of the possible structural alterations in order to assess the concomitant variations in the Raman matrix elements governing the signal intensities. Here we are set to investigate the microscopic mechanisms leading to the appearance of SHG in "thermally" poled glasses using neutrons as a probe. Alterations in the microscopic structure are explored by diffraction means, whereas the perturbations of the microscopic dynamics are addressed by means of inelastic neutron scattering (INS) measurements of the generalized frequency spectrum.

The samples were made of electrically-fused quartz (Infrasil, Heraeus) with dimensions $40 \times 40 \times 0.1$ mm³. The thickness ($\sim 100\mu\text{m}$) was chosen as the smallest possible, in order to increase the poled/unpoled volume ratio. In fact, after treatment [4], the nonlinearity is confined to a region $\sim 5\mu\text{m}$ deep under the anode surface regardless of the sample thickness. Poling was carried out at 548 K under an applied dc voltage of ~ 5 kV for 40 minutes. The poled sample consisted in fifteen plates stacked together. For comparison a similar stack of unpoled samples was used. The measurements were performed using the LAD, time-of-flight diffractometer and the MARI spectrometer, both at the ISIS pulsed neutron source (R.A.L., UK). Those carried out at the diffractometer sought to detect indications of local anisotropy induced by poling. To see this, sets of two runs with the samples oriented $\pm 45^\circ$ with respect to the incident

beam, were performed. The diffractometer consists in an array of 14 neutron counters covering a 2π angular range at discrete intervals each one spanning a large extent of momentum-transfers. In particular, our interest will here be focused on the analysis of those detectors $\pm 90^\circ$ with respect to the incident beam which span momentum-transfers covering directions mostly normal and parallel to the plates. Two spectra for both directions of momentum-transfers are then obtained with the corresponding detectors interchanged (see inset in Fig. 1). In doing so, exploration along the direction of the field applied during poling and normal to it is envisaged. After averaging over both orientations, systematic errors are minimized.

The experimentally-accessible quantity of interest is here the static pair correlation function $d_{\parallel,\perp}(r)$ or alternatively, the radial distribution function $g_{\parallel,\perp}(r)$, both related to the observable static structure factor $S(Q)$ by a sine-Fourier transform, $d_{\parallel,\perp}(r) = 4\pi\rho r[g_{\parallel,\perp}(r) - 1] = \frac{2\pi}{Q} \int dQ Q(S_{\parallel,\perp}(Q) - 1) \sin(Qr)$. The subscripts refer to directions parallel or normal to the stack of plates and ρ stands for the average number-density of the glass. The $d_{\parallel,\perp}(r)$ contains information about the thermally-averaged distribution of interatomic distances. For low values of r one expects to find sharp peaks corresponding to distances separating directly bonded atoms, such as Si–O or those O–O, which result from a pair of atoms linked to a common Si nucleus. At larger distances the structure is progressively washed out because of the static disorder and no measurable hints of ordering are expected well beyond some 20 Å.

The Fig. 1 depicts the $g_{\parallel,\perp}(r)$ functions measured for the poled plates and compared to that obtained for the native glass. A glance to the curves drawn there reveals a large difference in static correlations of the poled samples between parallel and perpendicular directions concerning distances within the 2.8–3.4 Å range. The graphs of the native samples serve to quantify any source of systematic error. The shortest distance, which corresponds to Si–O bonds, appears at 1.6175 (6) Å and that regarding O–O correlations shows up at 2.641 (1) Å. The differences between measurements mostly parallel and normal to the native glass plates are very small (differences in peak position of 2×10^{-3} Å and 7×10^{-3} Å in width). In contrast, the curves for the poled samples show that: (a) $g_{\parallel}(r)$ is basically unchanged after poling, (differences in the peak center and linewidth are, within the error bars indistinguishable from those of the unpoled plates), (b) $g_{\perp}(r)$ of the poled glass shows a peak at distances characteristic of Si–Si correlations significantly wider than that of the native sample, and (c) clear hints of a bimodal distribution of Si–Si distances are seen in the latter function. In other words, the difference between $g_{\parallel}(r)$ and $g_{\perp}(r)$ unequivocally shows the presence of an exceedingly strong anisotropy at scales of about 3 Å, which correspond to Si–Si correlations, that is, to distances between the centers of neighboring tetrahedra. More specifically, after a decomposition of the $g_{\parallel,\perp}(r)$ functions below 5 Å into a sum of Gaussians, the Si–Si peak appears in the native sample centered at 3.060 (9) Å with a width of 0.115 (8) Å in both \parallel and \perp directions. The peak shape of the same feature in $g_{\perp}(r)$ for the poled plates can be reproduced by addition of a further Gaussian which is now centered at 3.228 (23) Å and has a width of 0.106 (8) Å. The ratio of the integrated intensities of these two peaks at high- and low- r is of 0.008/0.140, that is about 5.7 per cent, a figure which becomes fairly close to the ratio of poled/unpoled material.

Some additional alterations in the glass structure are revealed in the difference function $\Delta d(r) = d_{\text{poled}}(r) - d_{\text{unpoled}}(r)$ between poled and unpoled samples, this time $d(r)$ being evaluated from an average taken over all detectors. There, a negative peak appearing at 4.4 Å merits to be commented on, since this corresponds to a real-space manifestation of a difference in height of the first diffraction peak which shows its maximum at $\approx 1.5 \text{ \AA}^{-1}$. The observed effects are commensurable with the increase in the Si–Si distance upon poling since Si–O, O–O and Si–Si correlations contribute to the first peak in $S(Q)$ with an in-phase oscillation in their partial structure factors, and therefore a mismatch of one of these correlations will lead to a decrease in the peak height.

The microscopic details of the structure within the poled region are difficult to access because of the weakness of the signals and the mechanism by which this happens can only be a matter of educated guessing. However, both the value of 3.22 Å of the Si–Si distance within the poled zone as well as the decrease in correlations about 4 Å provide indications of a structure more open than that of the native glass which arises in the direction perpendicular to the plate surface as a consequence of poling. The value for the Si–O–Si bond angle would then reach some 167° , which although far larger than that of 142° of the unpoled glass sits within the range of values found for some polymorphs of SiO₂ (see Table I of [12]). On the other hand, most of the known structures of the disordered phases of SiO₂ show fairly wide distributions for the referred angle, meaning that values as large as that quoted above still have a very substantial probability of occurrence (see for instance Fig. 5 of [11]).

The possibility of inducing a transformation from the isotropic glass to a less disordered form can be understood on the basis of recent results [14], which show how disordered crystal phases can be formed from a glassy (or deeply supercooled) state. In the particular case of silica polymorphs a common parent structure corresponding to a disordered b.c.c. crystal can be found, from where the known forms of SiO₂ can be derived [13] by ordering and displacive mechanisms which involve pressure and the degree of occupancy of the b.c.c. structure by oxygen atoms. It seems then plausible to expect an ordering transition between the fully disordered and some partially ordered structure occurring

via the referred cubic crystal as a consequence of the aligning electric-field. Large scale particle rearrangements within the glassy matrix can be expected to occur under the harsh conditions of poling. A glaring example of this is provided by the recent observation of full crystallization after segregation towards the surface of some of the components of soda-lime silicate glass-plates as a consequence of poling under conditions very close to those herein employed [6].

The resulting structure may share some characteristics with some of the disordered crystalline polymorphs of SiO_2 such as *beta*-cristobalite since: (a) the density of the latter is very close to that of the glass, so that a transformation at ambient pressure can be envisaged, (b) the poling field is applied at temperatures where the β -cristobalite structure becomes the stable crystalline form at such density, and c) the rather open Si–O–Si bond angle is also reminiscent of that proposed time ago for an idealized structure of high-temperature cristobalite, a form which although dynamically unstable [12] may possibly exist quenched within the glass after the poling field is removed.

The $Z(\omega)$ frequency spectrum (vibrational density of states), has been measured using incident energies of 220 meV and 150 meV in order to cover kinematic ranges with different resolution in energy-transfers. To pursue the derivation of $Z(\omega)$ from the measured data, the procedure described in Ref. [7], was followed. It consists in an iterative scheme designed to correct for a number of instrumental and sample-dependent (multiphonon) effects for coherently-scattering materials, and has been shown to give results in good agreement with thermodynamics [7]. The same procedures were followed to derive the spectra for both poled $Z_p(\omega)$ and native $Z_u(\omega)$ materials. Therefore, the $Z_p(\omega) - Z_u(\omega)$ difference function should be free of systematic errors. Measurements along different directions as done at the diffractometer are here far more complicated so that only an angular average was considered.

The Fig. 2 displays a comparison between the distributions for native and poled samples up to 120 meV ($\approx 960 \text{ cm}^{-1}$). The spectra show as main features a low frequency region (limited by resolution effects) with a shoulder at 20 meV, a maximum at about 53 meV and a narrow peak at 100 meV. Additional structure appears at higher frequencies, such as the well known double peak with maxima at 135 meV ($\approx 1080 \text{ cm}^{-1}$) and 150 meV ($\approx 1200 \text{ cm}^{-1}$) meV. The frequencies explored here comprise those where previous Raman studies found changes induced by poling. In spectra shown in Fig. 2, a measurable difference between poled and unpoled glasses is seen for a band comprising 60 meV ($\approx 480 \text{ cm}^{-1}$) $\leq \omega \leq 95 \text{ meV}$ ($\approx 760 \text{ cm}^{-1}$) and for the shape of the peak at 100 meV ($\approx 800 \text{ cm}^{-1}$). The differences, especially on the band about 60 meV have to be regarded as rather large, account made of the fact that the strong effect expected on the basis of the large anisotropy seen by diffraction is here averaged. The observed changes comprise those seen in previous Raman studies [5], and therefore, our results indicate that the alterations, as seen in the dynamics, are far more widespread than previously reckoned. The measurements carried out using a larger incident energy (220 meV) confirmed the above mentioned changes and enabled the exploration of the spectral region extending up to 180 meV ($\approx 1440 \text{ cm}^{-1}$) which comprises the strong double-peak structure referred above [9]. No significant changes upon poling were found within that range of frequencies.

The assignment of features in $Z(\omega)$ to microscopic “modes” still is a matter of debate. A rationalization could be pursued in terms of models developed to describe the high-frequency Raman spectrum [8]. Accordingly, the broad peak about 53 meV would correspond to the so called ω_1 mode, where the oxygens undergo a symmetric stretch whereas the Si atoms stand still. That appearing at ≈ 100 meV is assimilated with the ω_3 mode, where all atoms move. The model is supplemented by two “defect” modes, introduced to explain the origin of the two narrow D_1 and D_2 Raman lines appearing at ≈ 61 meV (495 cm^{-1}) and ≈ 75 meV (606 cm^{-1}) (see inset of Fig. 2). Their origin is sometimes ascribed to the presence of intermediate-range-order. A schematic drawing of the polarized (HH) Raman response from vitreous silica is shown in the inset of Fig. 2 for comparison purposes. From the diffraction results, one then expects changes in the frequency ranges associated with variations in intermediate-range order because the latter has been altered. This is indeed the case since the D_1 and D_2 lines are within the region where clear differences between poled and unpoled spectra are seen. On the other hand, the narrowing of the 100 meV peak can be plausibly attributed to a reduction in the spread of inter-tetrahedral angle [10], for which some hints are also provided by the diffraction results.

On the basis of the previous discussion about the structural modification, a comparison with results regarding the spectra of highly disordered silica polymorphs [11], seems adequate. That concerning the strongly disordered cubic phase of β -cristobalite shows a broad maximum at about 62 meV [11]. The increase in intensity within the $65 \text{ meV} \leq \omega \leq 90 \text{ meV}$ frequency interval, seen upon poling would then be compatible with the emergence within the poled region of a structure somewhat reminiscent of that for the alluded polymorph.

In summary, large microscopic alterations are found in fused silica after the material is subjected to “thermal poling”. These result in the breakdown of isotropy occurring within the glass which involves at least next-nearest neighbors. Such directional ordering along the direction of the poling field has, as a direct dynamical consequence, the alterations comprising a range of frequencies between 65 meV and 100 meV seen in the vibrational density of states. Whether such alterations can account for the measured optical second order nonlinearity needs to be clarified possibly by computational means for which the collected data constitutes an invaluable benchmark.

ACKNOWLEDGMENTS

Work supported in part by grants No. TIC95-0563-C05-03, No. PB96-00819, CICYT, Spain, and Comunidad de Madrid 06T/039/96. V. Pruneri acknowledge Pirelli Cavi (Italy) for his fellowship.

- [1] U. Osterberg and W. Margulis, Opt. Lett. **11**, 516 (1986).
- [2] A. Yariv and P. Yeh, *Optical waves in crystals*, Wiley, 1984, p. 504.
- [3] E.M. Dianov *et al.*, Sov. Lightwave Commun. **1**, 247 (1991); D.Z. Anderson, *et al* Opt. Lett. **16**, 796 (1991).
- [4] R. A. Myers *et al*, Opt. Lett. **16**, 1732 (1991).
- [5] J.M. Gabriagues and H. Fevrier, Opt. Lett. **12**, 720 (1987); A. Kamal *et al*, Opt. Lett. **15**, 613 (1990); I.V. Alekandrov *et al*, J. Non-Cryst. Solids, **167**, 117 (1994).
- [6] M. Qiu *et al.*, J. Opt. Soc. Am. B**15**, 1362 (1998).
- [7] J. Dawidowski *et al.*, Phys. Rev. E **53**, 5079 (1996).
- [8] M.F. Thorpe in *Excitations in disordered systems*, Plenum New York, 1982, p. 85.
- [9] J.M. Carpenter and D.L. Price, Phys. Rev. Lett. **54**, 441 (1985).
- [10] F.L. Galeener in *Disorder in Condensed Matter Physics*, J.A. Blackman and J. Tagüeña (Eds.), Oxford Science Publications, The Clarendon Press, Oxford, 1991, p. 45.
- [11] I.P. Swainson and M.T. Dove, J. Phys. C **7**, 1771 (1995).
- [12] P. Vashista *et al*, Phys. Rev. B**41**, 12197 (1990).
- [13] V. Dmitriev *et al*, Europhys. Lett. **37**, 553(1997).
- [14] R. Fayos *et al.*, Phys. Rev. Lett. **77**, 3852 (1996).

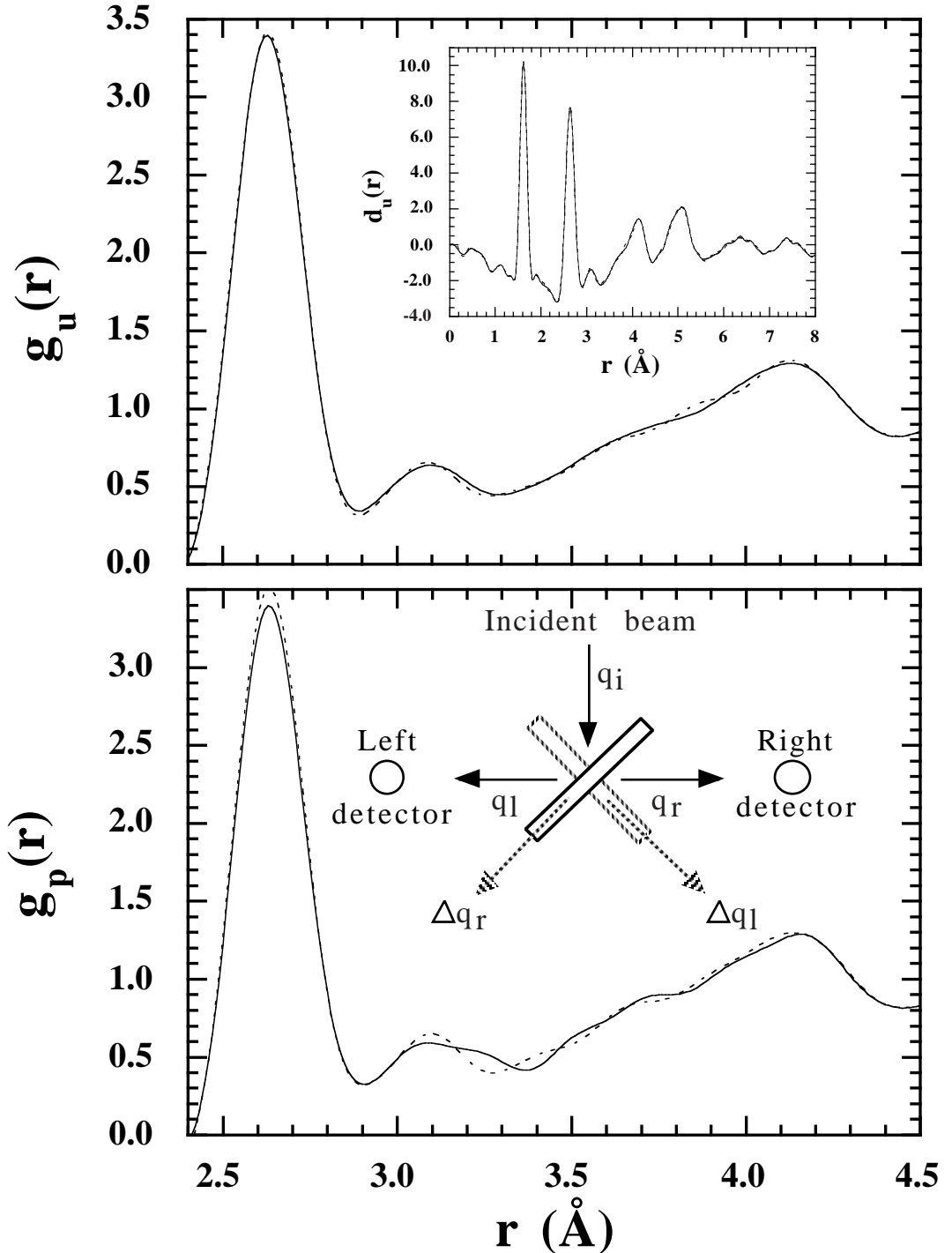


FIG. 1. A comparison between the functions $g_{\parallel}(r)$ (dotted line) and $g_{\perp}(r)$ (solid line) f111 or both, the native (upper figure) and the poled samples (lower figure). The inset in the upper figure displays the whole measured $d_{\parallel,\perp}(r)$ while the inset in the lower figure shows the detectors/sample geometry.

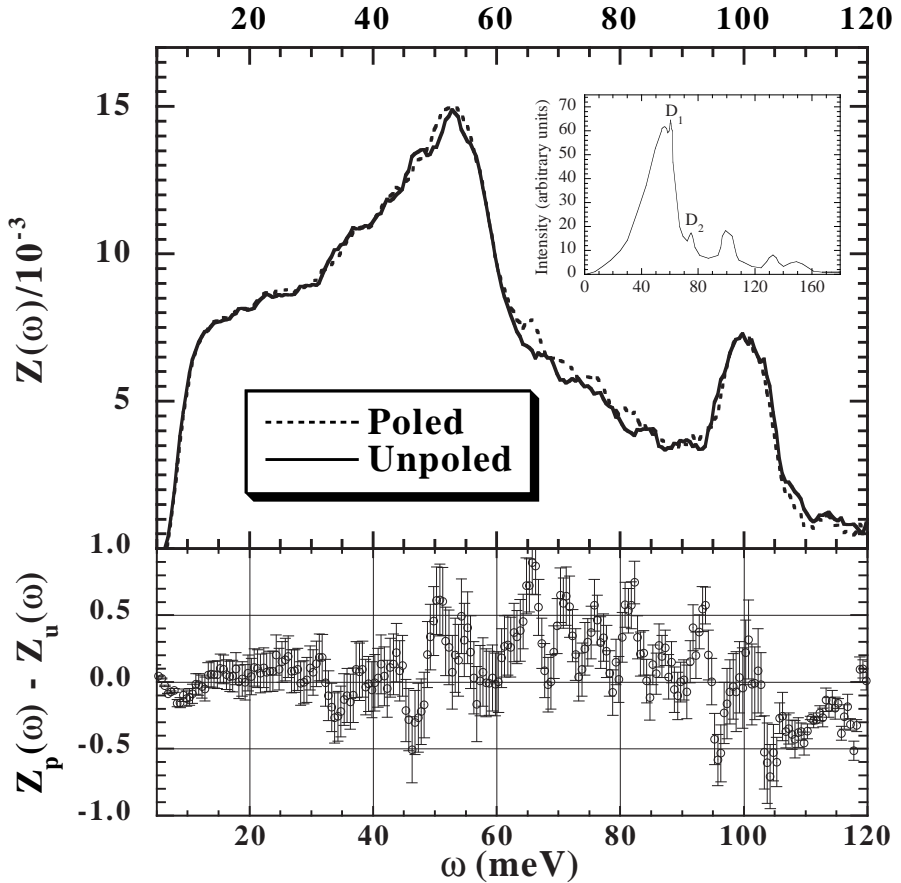


FIG. 2. The $Z(\omega)$ frequency distribution of both, the native (solid line) and poled (dashed line) samples and the difference between them. Error bars in $S(\omega)$ ($\sigma_S(\omega)$) are proportional to the square root of the number of counts in each detector. For the DOS, the error bars are obtained taking the semidifference between the DOS calculated with $S(\omega) + \sigma_S(\omega)$ and $S(\omega) - \sigma_S(\omega)$ as input. After a smoothing process over five points, the error was divided by $5^{1/2}$. The inset depicts a schematic representation of the HH-polarized Raman spectrum of bulk v-silica, showing the location of the D_1 and D_2 defect modes.